

Preparation and Characterization of Folic Acid Linked Poly(L-glutamate) Nanoparticles for Cancer Targeting

Yong-kyu Lee*

Department of Chemical and Biological Engineering, Chungju National University, Chungbuk 380-702, Korea

Received March 22, 2006; Revised May 15, 2006

Abstract: Nanoparticles of Poly(L-glutamic acid) (PG) conjugated to the anticancer drug paclitaxel and targeted moiety folic acid (FA) were synthesized and characterized *in vitro*. The nanoparticles were designed to take advantage of FA targeting to folate receptor (FR) positive cancer cells. The chemical composition of the conjugate was characterized by ¹H-NMR, FTIR and UV/vis spectroscopy. The selective cytotoxicity of the FA-PG-paclitaxel conjugates was evaluated in FR positive cancer cells. The interaction of the conjugate was visualized by fluorescence microscopy with results confirming the successful preparation of the conjugate and the production of nanoparticles of about 200-300 nm in diameter. The amount of paclitaxel conjugated to FA-PG was 25% by weight. Cellular uptake of the conjugate was FA dependent, and the conjugate uptake was mediated specifically by the folate receptor. These results demonstrate the improved selective toxicity and effective delivery of an anticancer drug into FR bearing cells *in vitro*.

Keywords: cancer targeting, folate receptor, nanoparticles, PG.

Introduction

Active targeted delivery of anticancer drugs is a promising approach towards the development of new drug carriers. By modifying the surface of nanoparticles with carefully designed water soluble polymers, several major improvements may be achieved, such as long circulation time and specific targeting.^{1,2} Especially, introducing targeting moieties to the polymer carriers will enhance the active targeting potential of the polymer-drug conjugates.^{3,4} Many researchers have studied several targeting ligands such as antibodies, cytokines, and homing peptides to improve the tumor selectivity of polymeric drug carriers.⁵⁻⁷ However, the attachment of an antibody or a homing peptide to polymeric carriers has met with limited success in animal studies. The reasons may be either changes of chemical properties due to functional group modification or decreased interaction with receptor due to embedding of target moieties in polymeric carriers.^{8,9}

Folic acid (FA) is a water soluble vitamin and a ligand used for tumor targeting via folate receptor (FR)-mediated endocytosis. FR is known to be abundantly expressed in a large fraction of human tumors, but only minimally distributed in normal tissues. Therefore, FR serves as an excellent tumor marker as well as a functional tumor-specific recep-

tor.^{10,11} So far, carboxyl groups of folic acid have been utilized as the site of conjugation with polymeric carriers or drug. Modification of the carboxyl group did not decrease the binding affinity of folic acid with FR positive cancer cells.¹¹ For amplification or multiplication of FA effects on a molecular level, a single polymeric chain may be conjugated with multiple ligands to enhance the binding affinity of the targeting moiety.¹² Polyvalent interactions can be much stronger than monovalent interactions, and they can provide the basis for mechanisms of both agonizing and antagonizing biological interactions that are fundamentally different from those available in monovalent systems.¹³⁻¹⁵ Especially, ligand-receptor interactions are important in cancer targeting to create high local concentrations of drugs around tumor cells. The high binding affinity also can reduce side effects such as hair loss, anemia, fatigue and interstitial pneumonia syndrome due to the high dose and unspecific binding of the anti-cancer drug.^{16,17}

One of the well-known water soluble paclitaxel conjugate published is poly(L-glutamic acid) (PG)-paclitaxel conjugate that has shown both anti-tumor effect and improved therapeutic index *in vivo*.¹⁸⁻²⁰ Paclitaxel was coupled by mainly ester bond to be released from the conjugated polymer when the conjugate reached the tumor cells. However, the lack of selectivity of PG-paclitaxel caused unspecific binding with proteins or enzymes.²¹ In this study, we synthesized FA-PG-paclitaxel conjugates which can potentially direct active

*Corresponding Author. E-mail: leeyk@chungju.ac.kr

agents to tumors and reduce toxic effects to normal tissues. Tumor cells tend to uptake the FA-PG-Paclitaxel conjugates after interaction with FR. Furthermore, selective delivery of anti-cancer drugs to cancer cells was achieved by receptor mediated endocytosis.

Experimental

Materials. Qdot™ 655 Streptavidin Conjugate (Quantum dot with emission maximum at 655 nm) was purchased from Quantum Dot Corp. (Hayward, CA). Paclitaxel was purchased from Hande Tech (Houston, TX). Poly(L-glutamic acid) (PG, Mw: 41,400 Dalton), *N*-hydroxysuccinimide (NHS), dicyclo-hexylcarbodiimide (DCC), FA, ethylene diamine (EDA), and pyridine were obtained from Sigma (Milwaukee, WI). Anhydrous diethyl ether, acetonitrile, formamide and dimethylsulfoxide (DMSO) were purchased from Merck (Darmstadt, Germany). Penicillin-streptomycin, fetal bovine serum (FBS), 0.25% (w/v) trypsin-0.03% (w/v) EDTA solution, EMGM medium and all cell lines were purchased from American Type Culture Collection (Rockville, MD). RPMI-1640 medium (without FA) was obtained from Invitrogen (Carlsbad, CA).

Synthesis and Characterization of FA-PG-Paclitaxel Conjugate. The key step in the synthesis of FA-PG-paclitaxel conjugate is the generation of an active site in the PG structure to bind with FA and paclitaxel, respectively. Reaction of PG with FA was performed following the activation of PG (1 mmol) by reacting with DCC (10 mmol) and NHS (12 mmol) in formamide at 4°C overnight. The activated PG-NHS (1 mmol) and aminated folate (10 mmol) were reacted at room temperature for 1 day. The amination of folate was conducted by using EDA. The unreacted NH₂-folate was removed by dialysis (MWCO 2000). The final yellowish product was obtained by freeze-drying. The yield of conjugation was 95%. After FA-PG conjugate (1 mmol) was dissolved in formamide, Paclitaxel (20 mmol) and DCC (20 mmol) in DMSO were added and reacted for overnight at room temperature. After the reaction, recrystallization and filtration were done to remove the unreacted DCC. For further purification, this product was precipitated by adding excess acetonitrile. After filtration, the yellow powder was dried in vacuum. The reaction was confirmed by TLC analysis (silica plate; eluent, 2-propanol/chloroform 10:90 vol%) and ¹H-NMR (400 MHz, in D₂O). Values For ¹H-NMR of FA-PG-Paclitaxel were: δ1.11 [s, ¹⁷CH₃], 1.20 [s, ¹⁶CH₃], 1.69 [s, ¹⁹CH₃], 1.97 [s, ¹⁸CH₃], 2.2 [m, OAc], 2.4 [m, OAc], 3.78 [d, ³CH], 4.17 [d, ²⁰CH₂], 4.27 ppm [H-α, PG], 4.3 [d, ²⁰CH₂], 4.39 [dd, ⁷CH], 4.96 [d, ⁵CH], 4.78 and 5.63 [d, ²CH], δ5.6 [COO between PG and Paclitaxel], 5.67 [d, ²CH], 5.98 [dd, ³CH], 6.22 [t, ¹³CH], 6.27[s, ¹⁰CH], δ6.64[d, 3', 5'-H of FA, 2H], 7.09 [d, NH], 7.25 [s, 3'-Ph], 7.4 [m, 3'-NBz], 7.5 [m, 2-OBz], 7.73 [d, 3'-NBz], 8.1 [d, 2-OBz], δ8.1-8.45 [CONH between PG and FA].

The content of paclitaxel conjugated to FA-PG was estimated by UV (Shimadzu UV-2401PC) measurements based on a standard curve generated with known concentrations of paclitaxel in methanol ($\lambda=228$ nm). The IR spectra of FA-PG-paclitaxel were acquired on a Fourier transform infrared spectroscopy (FTIR) using a Perkin Elmer system 2000 spectrometer and the samples were analyzed as KBr pellets. The average particle size, size distribution and morphology were examined using a particle size analyzer (Malvern Instruments Co., zetasizer 3000, spring lane, UK) and samples for the size measurements were prepared by dispersing small amounts of the FA-PG-paclitaxel powder in water and treating in an ultrasonic bath for 1 min.

In Vitro Studies with Tumor and Normal Cells: Selectivity, Cytotoxicity, and Imaging. MCF-7 (Human breast cancer cells) and MCF-10A (normal human breast cells) were used because of the positive FR overexpression (MCF-7) or the lack of a detectable FR expression (MCF-10A). The MCF-7 cell lines were cultured at 37°C in a humidified atmosphere containing 5% CO₂ in FA deficient medium RPMI 1640 with 10% fetal calf serum. The MCF-10A cell lines were cultured at 37°C in a humidified atmosphere containing 5% CO₂ in medium MEGM (Mammary epithelial growth medium, serum-free) supplemented with cholera toxin. The cells (5×10⁴ cells/mL) grown as a monolayer were harvested by 0.25% trypsin-0.03% EDTA solution. The cells (200 μL) in their respective media were seeded in a 96-well plate and preincubated for 24 h before the assay.

For studying selectivity and cytotoxicity of FA-PG-paclitaxel, MTT assay was performed on MCF-7 cells and MCF-10A cells by incubating at 37°C for 2 days. The control was incubated at 37°C for 2 days without adding a drug. For MTT assay, five different concentrations (0.1, 1, 10, 50 or 100 ng/mL) of the each compound was used. This assay is based on the reduction of the yellow tetrazolium component (MTT) to an insoluble purple-colored formazan produced by the mitochondria of viable cells. After a 48 h incubation, 100 μL of medium containing 20 μL of MTT solution was added to each well and the plate was incubated for an additional 4 h, followed by the addition of 100 μL of MTT solubilization solution (10% Triton X-100 plus 0.1 N HCl in anhydrous isopropanol, Sigma, Milwaukee, WI) to each well. The solution was gently mixed to dissolve the MTT formazan crystals. The absorbance of each well was read with a microplate reader at a wavelength of 570 nm. The background absorbance of well plates at 690 nm was measured and subtracted from the 570 nm measurement. Statistical analysis was done using ANOVA. *p*<0.01 was accepted as statistically significant. Error bars represent standard error of mean (SEM).

For studying cellular interaction and imaging of FA-PG-paclitaxel conjugates, fluorescence microscopy (Leica, Germany) was performed with MCF-7 cells grown on a Lab-

Tek® II chamber slide (Nalge Nunc, Naperville, IL). Paclitaxel-7-O-biotin (Hande Tech) was conjugated with Qdot 655 Streptavidin and purified by centrifuging to remove unreacted paclitaxel-7-O-biotin. The concentration of FA-PG-paclitaxel-Qdot655 conjugates was 1 $\mu\text{g}/\text{mL}$ in RPMI-1640 medium. After 1 h incubation, the medium containing the complexes was aspirated from the wells. The cells were then washed three times with PBS buffer (pH 7.4) and finally 200 μL of 4% formaldehyde in phosphate buffer saline was added. The samples were observed as quickly as possible. Initial scanning of the tissue sections was done under low power magnification (10 \times).

Results and Discussion

FA-PG-Paclitaxel Conjugate. The conjugation between FA and PG was achieved by founding amide bonds formed by coupling between carboxyl groups of PG and amine groups of aminated FA. To aminate FA, FA (1 mmol) dissolved in 30 mL DMSO was reacted with DCC (1 mmol) and NHS (2 mmol) at 60°C for 8 h. The pure FA-NHS was obtained by filtering the precipitated DCU. The resulting FA-NHS was mixed with ethylene diamine (100 mmol) and 200 μL pyridine and allowed to react at room temperature overnight. The reaction was confirmed by TLC analysis (silica gel plate, 2-propanol/chloroform, 70:30 v/v%). The crude product was precipitated by addition of excess acetonitrile, filtered and washed three times with diethyl ether before drying under vacuum. For further purification, this product was dissolved in 2 N HCl and precipitated by adding an excess volume of acetonitrile. After filtration, the fine dark yellow powder was dried in vacuum. The unreacted FA and diaminated FA (FA-(NH₂)₂) were separated by ion-exchange chromatography. The column (10 \times 200 mm) was packed by swollen DEAE Sephadex A-25 in 0.5 M potassium tetraborate solution (pH 7.0). After dissolving in 30 mL of deionized water, the product (0.03 mg/mL) was loaded into the column. The linear ionic gradient of ammonium bicarbonate solution (pH 7.8, 10 to 30 mM) was applied. The FA-NH-(CH₂)₂-NH₂ solution was fractionally collected after continuous TLC analysis as mentioned above. The aminated FA solution was evaporated. The remained α mono-aminated FA [α FA-NH-(CH₂)₂-NH₂] and γ mono-aminated FA [γ FA-NH-(CH₂)₂-NH₂] can be included in the final products. The presence of peaks at δ 4.27 ppm in the ¹H-NMR spectrum data confirmed that γ -carboxyl group in folic acid was primarily modified by EDA. The synthesis of the FA-PG was confirmed by the presence of peaks at δ 6.75-8.77 ppm in the ¹H-NMR spectrum of FA-PG and by an absorbance at λ =280 nm in the UV spectrum of the FA-PG. The presence of peaks at δ 4.27 ppm in the ¹H-NMR data confirmed that γ -carboxyl group in folic acid was primarily modified by EDA. These results are in accordance with other groups' studies that have shown γ -carboxyl group

is more reactive than the α -carboxyl group in folic acid.^{22,23} Coupling of the paclitaxel to FA-PG was achieved via a DCC mediated reaction of hydroxyl groups of paclitaxel and the carboxyl groups of PG. The success of the linkage was confirmed by the presence of signals at δ 5.6 ppm in the ¹H-NMR spectrum. From the results, the specific site of esterification between paclitaxel and PG may have occurred at both the C-2' and C-7 positions because unsubstituted C-2' peaks of paclitaxel still remained. Li *et al.* also reported the binding site of paclitaxel with PG could be done at both the C-2' proton and C-7 positions.²³ From the FTIR spectrum, the binding between FA-PG and paclitaxel was confirmed by the decrease of peak intensity around at 3280-3400 cm⁻¹ (O-H bond) in FA-PG-paclitaxel. The UV spectrum of FA-PG-paclitaxel conjugate in water had slightly shifted (λ_{max} =210 nm) as compared with that of paclitaxel in methanol (λ_{max} =228 nm). The UV spectrum of free FA was determined at 280 nm, indicating no overlapping with paclitaxel curve. For the conjugate, we also found that the intensity of shift curve to 210 nm was changed with concentration of FA-PG-paclitaxel conjugate. Therefore, there is no problem to obtain amount of conjugated paclitaxel in FA-PG-paclitaxel at 210 nm. The solubility of FA-PG-paclitaxel in water

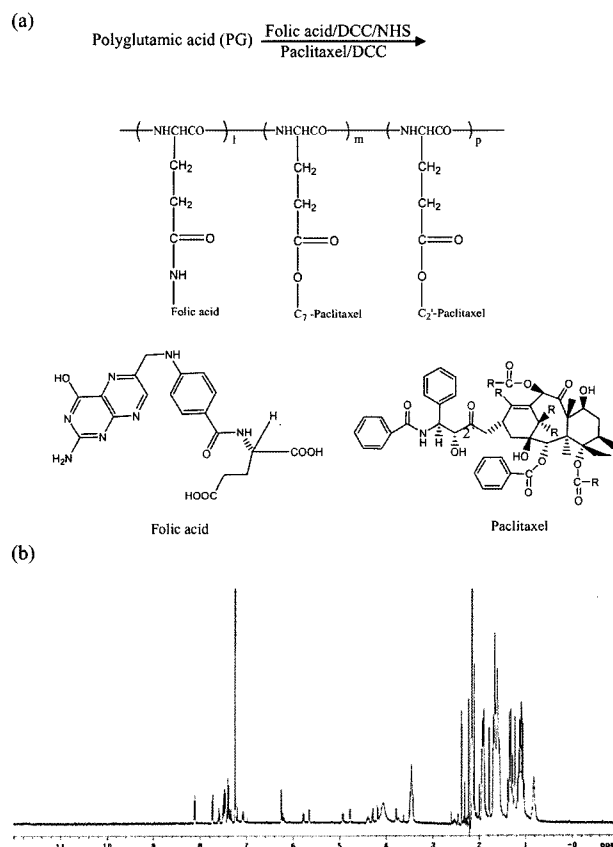


Figure 1. (a) Structure of FA-PG-paclitaxel conjugate, folic acid, and paclitaxel, and (b) FT-NMR of FA-PG-paclitaxel conjugate.

produces a clear solution in the concentration of 80 mg/mL. The amount of paclitaxel conjugated to FA-PG was 25.6% by weight estimated by UV spectrums based on a standard curve.

Figure 2 shows the size distribution and shape of FA-PG-paclitaxel conjugate by dynamic light scattering (DLS) and transmission electron microscopy (TEM), respectively. TEM micrograph of FA-PG-paclitaxel conjugate was taken to determine the shape and uniformity of the particles as shown in Figure 2(a). The picture shows that the particles have a uniform spherical shape. The mean diameter of the nanoparticles was 300 nm with a standard deviation of 10.1 nm (This standard deviation was obtained by measuring same sample three times). From TEM, we found that particle size of dried nanoparticles was decreased to 50-200 nm. This difference might be caused by a hydrodynamic volume

of FA-PG-paclitaxel conjugate in aqueous solution. We also measured the size distribution of free paclitaxel in water after ultrasonication for 3 min. The average size of free paclitaxel was 4399 nm with a standard deviation of 263 nm in diameter (data not shown).

The ability of paclitaxel and FA-PG-paclitaxel conjugate to induce microtubule assembly *in vitro* was determined at 10 μ M paclitaxel or FA-PG-paclitaxel conjugate. The addition of paclitaxel to a solution of tubulin in an assembly buffer caused a clear increase in absorbance due to the increase in light scattering that resulted from the polymerization of tubulin into microtubules. On the other hand, 10 μ M paclitaxel equivalent of FA-PG-paclitaxel had no effect on the polymerization (data not shown). The ability of paclitaxel to induce microtubule assembly dramatically decreased after modifying hydroxyl group in paclitaxel struc-

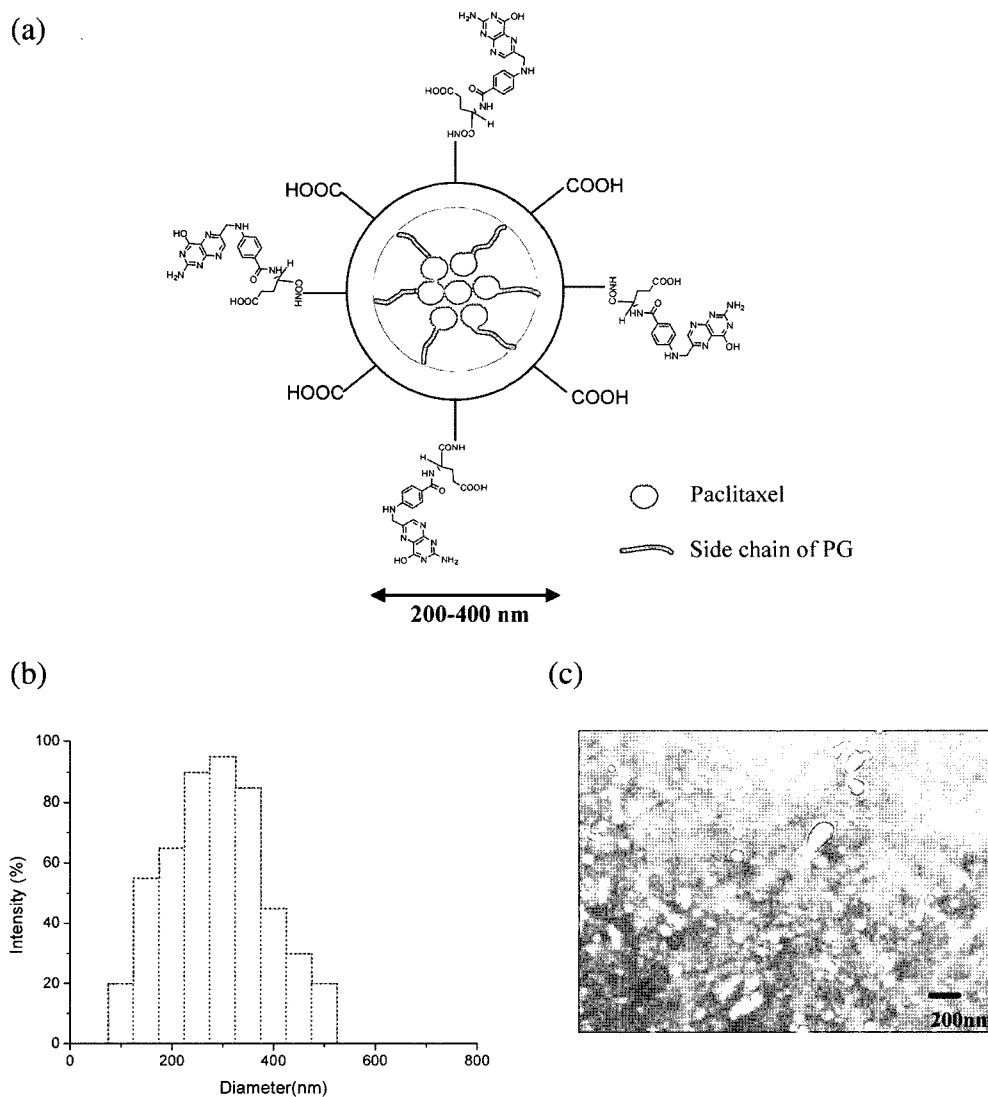


Figure 2. Characterization of FA-PG-paclitaxel conjugate. (a) schematic structure of FA-PG-paclitaxel nanoparticles, (b) size distribution of FA-PG-paclitaxel conjugate, and (c) TEM image of the nanoparticles.

ture.

In the comparison of fluorescence intensity of Qdot and FA-PG-paclitaxel-Qdot, the modified Qdot showed a similar intensity with unmodified Qdot. It means that Qdot intensity may not be influenced by conjugation with polymeric carrier (data not shown).

Selectivity of FA-PG-Paclitaxel Conjugate *in vitro*. MCF-7 cells (FR positive cancer cells) and MCF-10A (FR negative normal cells) were used to determine the selective toxicity of FA-PG-paclitaxel conjugate by MTT assay. Figure 3(a) clearly showed different cell viability dependent on drugs, indicating significant decrease of selective toxicity with paclitaxel. The IC_{50} dose for FA-PG-paclitaxel conjugate in normal cells was not determined in the range of 0.1–100 ng/mL concentration. On the other hand, free paclitaxel showed significant increase in cytotoxicity and showed an IC_{50} of ≥ 100 ng/mL in normal cells. From the results, it is evident that FA plays a key role in markedly decreasing the cytotoxicity to normal cells. Interestingly, the cytotoxicity of

free paclitaxel on MCF-7 cells did not decrease compared to MCF-10A cells. In the range of 0.1 and 100 ng/mL concentration, both free paclitaxel and FA-PG-paclitaxel conjugate showed above 45% cell viability. After treated with high concentration of FA-PG-paclitaxel conjugate, the cell viability of MCF-7 cells decreased to around 50% as shown Figure 3(b). The targeted FA-PG-paclitaxel conjugate that can enter the FR positive cancer cells by receptor-mediated endocytosis have shown similar IC_{50} values with paclitaxel at 1,000 ng/mL concentration (data not shown). In normal cells, the reduction in cytotoxicity is best explained by the formation of self assembled nanoparticle which conjugated paclitaxel is embedded inside of FA-PG-paclitaxel nanoparticle. In FR positive cancer cells, the effect of FA-PG-paclitaxel can be explained as follows; when not utilizing any receptors for uptake, the cell membrane has limited permeability to macromolecules unless active drug is released in free form from the polymer carrier. The exposed FA on the surface of the nanoparticle can easily interact with the FR of the cancer cell. After binding with FR, the nanoparticle or free paclitaxel can diffuse into the cytosol and the nucleus. Further investigation into the mechanism of cytotoxicity reduction may be needed. For a long incubation time (48 h), the cytotoxic effect of FA-PG-paclitaxel on cancer cells might be similar with that of free paclitaxel because free paclitaxel directly attack the cancer cell. Clearly, we have observed that FA-PG-paclitaxel can penetrate into the cells effectively in a short incubation time. We have also observed FA receptor binding competition with different free FA concentrations *in vitro*.

We also confirmed the selective cytotoxicity of FA-PG-paclitaxel conjugate from trypan blue assay. As illustrated in Figure 4, MCF-7 cells treated with 100 ng/mL of FA-PG-paclitaxel conjugate were stained to blue-colored dye which means the cells were non-viable. On the other hand, most of MCF-10A cells did not stain blue-colored dye after treatment with FA-PG-paclitaxel conjugate, suggesting selective cytotoxicity dependent on cell types. It suggested that the interaction of FA-PG-paclitaxel conjugate with FR positive cells was FR-mediated endocytosis. The role of FR in this study is further confirmed by the fact that FA-PG-paclitaxel conjugate could not interact with FR negative cells.

We examined the hydrolysis of FA-PG-paclitaxel after incubation at 37°C with time interval by HPLC. From the results, two peaks (retention time: about 3 and 14 min) of FA-PG-paclitaxel were shifted to the right at 18 min (pure taxol peak) after 7 days incubation. Even though we confirmed the hydrolysis of FA-PG-paclitaxel, it is hard to determine the exact amount of free paclitaxel by HPLC.

Imaging of Cell Binding of FA-PG-Paclitaxel Conjugate. For imaging of cell binding and uptake of the targeted FA-PG-paclitaxel conjugates, Qdot 655, Qdot 655-paclitaxel conjugate, FA-PG-paclitaxel-Qdot 655 conjugate were used to evaluate the degree of binding with MCF-7 and KB cells,

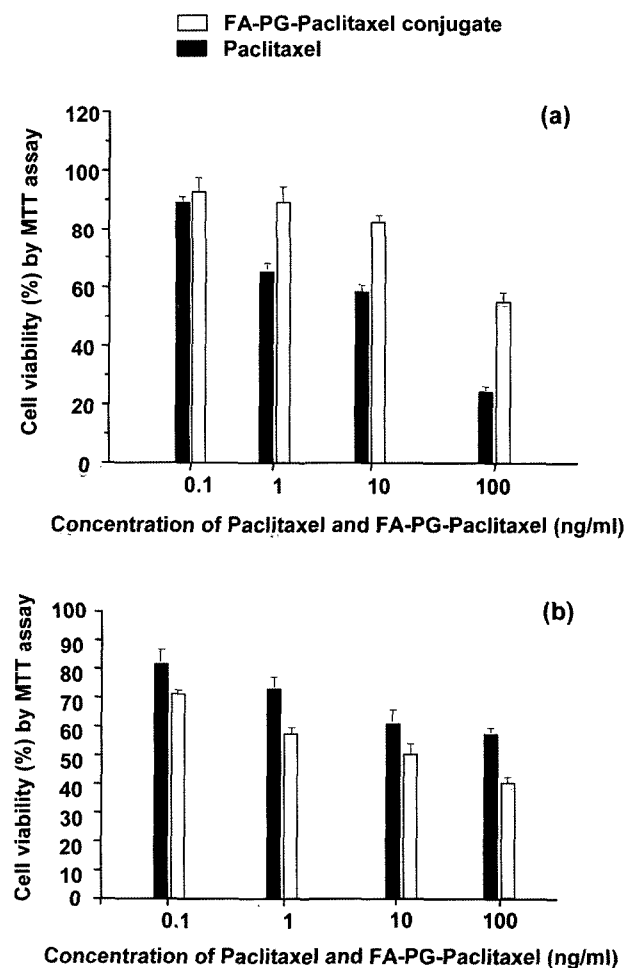


Figure 3. Cell viability of (a) MCF-12A cells (normal breast cells) and (b) MCF-7 cells (breast cancer cells) after treating paclitaxel and FA-PG-paclitaxel for 48 h incubation, respectively (n=4).

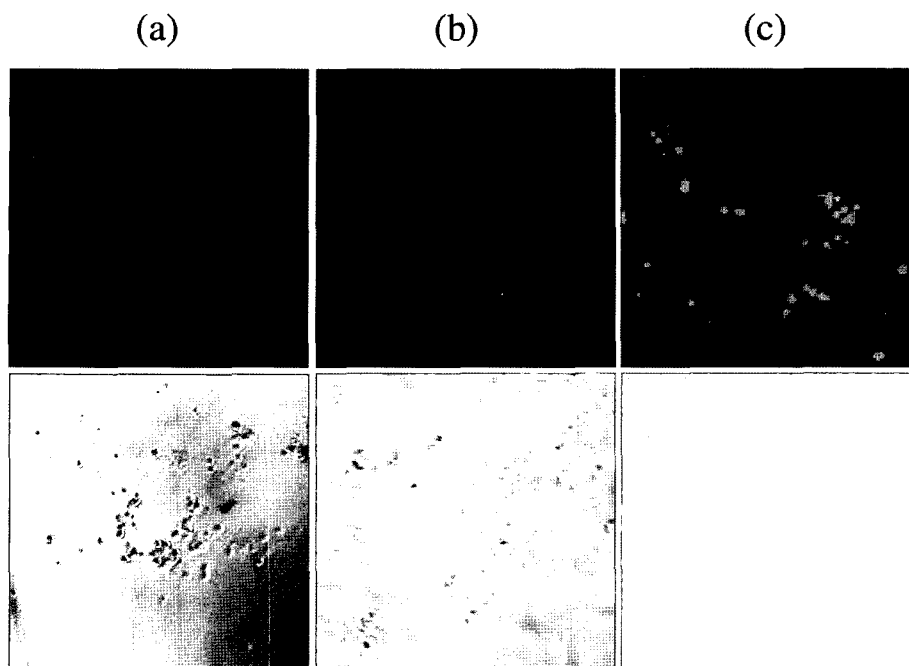


Figure 4. Microscopy data on MCF-7 cells after treating with (a) Qdot, (b) Qdot-paclitaxel, and (c) FA-PG-paclitaxel-Qdot. The pictures of the top row are obtained from overlay between optical and confocal image. The bottom row is confocal images of cells.

respectively. The advantages of Qdot in imaging are the follows: To see the interaction between folic acid and cell surface in a real time, Qdot should be conjugated to paclitaxel since Qdot is more stable in a long time under a light source compared to fluorescent dyes. In general, organic dyes such as FITC or RITC have a photobleaching and low Qdot yield. Therefore, we can not observe cell imaging with same fluorescent intensity. Another one is that can be used in animal experiment. All present organic dyes are broken and loose fluorescent intensity immediately *in vivo* while Qdot maintain the intensity longer. It is known that the KB cells used for these studies expressed approximately 4 million FA receptors per cell.²⁴ In comparison to the MCF-7 cells, confocal fluorescence images of FA-PG-paclitaxel-Qdot 655 conjugate uptake by KB cells showed a very strong fluorescence as shown in Figure 4. In non-targeted Qdot 655-paclitaxel conjugate, fluorescence intensity dramatically decreased. It suggests that the uptake of FA-PG-paclitaxel-Qdot 655 conjugate depend on the degree of FR expression in cancer cells. It also showed that endocytosis occurred in a rapid FR mediated pathway. To show significant selective cytotoxicity, FA-PG-paclitaxel conjugates have to be taken up by the cells via FR positive receptor and then release of free active paclitaxel by lysosomal enzymatic cleavage of the ester bond. We conclude that an active tumor targeting approach using receptor ligands coupled to nanoparticles can increase tumor specificity and decrease the required dosage *in vivo*.

Conclusions

In this study, we have prepared active targeting nanoparticles by using folic acid and have showed advantages over simple diffusion of drug into cancer cells. This strategy can be used to design active targeted delivery using receptor mediated endocytosis. This active targeted delivery takes advantage of the enhanced permeability and retention (EPR) effect. By introducing a targeting moiety to the self assembled nanoparticles, we could increase the therapeutic index through receptor mediated uptake by cancer cells. Furthermore, it increased the selective cytotoxicity of FA-PG-paclitaxel conjugate in FR positive KB or MCF-7 cells. *In vivo* study on the toxicity of FA-PG-paclitaxel conjugate is being conducted in this lab. Preliminary results indicate that the selective cytotoxicity of the conjugate in non tumor bearing mice increased markedly after injection of FA-PG-paclitaxel conjugate.

Acknowledgements. This study was supported partially by the Post-doctoral Fellowship Program of Korea Science & Engineering Foundation (KOSEF).

References

- (1) J. B. Gibbs, *Science*, **287**, 1969 (2000).
- (2) D. Dube, M. Francis, J.-C. Leroux, and F. M. Winnik, *Bioconjugate Chem.*, **13**, 685 (2002).
- (3) J. Sudimack and R. J. Lee, *Adv Drug Del. Rev.*, **41**, 147 (2000).
- (4) A. Tang, P. Kopeckova, and J. Kopecek, *Pharm. Res.*, **20**,

- 360 (2003).
- (5) M. V. Backer and J. M. Backer, *Bioconjugate Chem.*, **12**, 1066 (2001).
- (6) N. K. Egilmez, Y. S. Jong, M. S. Sabel, J. S. Jacob, E. Mathiowitz, and R. B. Bankert, *Cancer Res.*, **60**, 3832 (2000).
- (7) C. J. Mathias, D. Hubers, P. S. Low, and M. A. Green, *Bioconjugate Chem.*, **11**, 253 (2000).
- (8) G. F. Rowland, G. J. O'Neill, and D. A. L. Davies, *Nature*, **255**, 487 (1975).
- (9) J. Vega, S. Ke, Z. Fan, S. Wallace, C. Charsangavej, and C. Li, *Pharm. Res.*, **20**, 826 (2003).
- (10) P. Caliceti, S. Salmaso, A. Semenzato, T. Carofiglio, R. Fornasier, M. Fermiglia, M. Ferrone, and S. Priol, *Bioconjugate Chem.*, **14**, 899 (2003).
- (11) S. Wang, R. J. Lee, C. J. Mathias, M. A. Green, and P. S. Low, *Bioconjugate Chem.*, **7**, 56 (1996).
- (12) K. Y. Lee, *Macromol. Res.*, **13**, 542 (2005).
- (13) L. L. Kiessling, J. E. Gestwicki, and L. E. Strong, *Curr. Opin. Chem. Biol.*, **4**, 696 (2000).
- (14) M. Mammen, S.-K. Choi, and G. M. Whitesides, *Angew. Chem. Int. Ed. Engl.*, **37**, 2754 (1998).
- (15) D. M. Spencer, T. J. Wandless, S. L. Schreiber, and G. R. Crabtree, *Science*, **262**, 1019 (1993).
- (16) C. R. Thomas and P. Bonomi, *Curr. Opin. Oncol.*, **2**, 359 (1990).
- (17) R. Komaki, J. B. Putnam, and J. D. Shin Cox, *Curr. Opin. Oncol.*, **9**, 156 (1997).
- (18) C. Li, *Adv. Drug. Deliv. Rev.*, **54**, 695 (2002).
- (19) C. Li, J. E. Price, L. Milas, N. R. Hunter, S. Ke, D.-F. Yu, C. Charsangavej, and S. Wallace, *Clin. Cancer Res.*, **5**, 891 (1999).
- (20) R. Duncan, *Nature Rev. Drug Discov.*, **2**, 347 (2003).
- (21) W. Tansey, S. Ke, X.-Y. Cao, M. J. Pasuelo, S. Wallace, and C. Li, *J. Control. Release*, **94**, 39 (2004).
- (22) T. J. Deming, *Nature*, **390**, 386 (1997).
- (23) C. Li, D. F. Yu, R. A. Newman, F. Cabral, L. C. Stephens, N. Hunter, L. Milas, and S. Wallace, *Cancer Res.*, **58**, 2404 (1998).
- (24) C. P. Leamon, S. R. Cooper, and G. E. Hardee, *Bioconjugate Chem.*, **14**, 738 (2003).